# Carderock Division, Naval Surface Warfare Center

Bethesda, Maryland 20084-5000



**CARDIVNSWC-TR-95/010** April 1995

Hydromechanics Directorate
Research and Development Report


# A Postswirl Propulsor for a Small Vehicle


by
Benjamin Y.-H. Chen
Carol L. Tseng





The main text of this report was presented at the
Symposium of Propellers/Shafting '94,
Virginia Beach, Virginia, 20-21 Sep 1994.




THIS PAGE INTENTIONALLY LEFT BLANK

UNCLASSIFIED

SECURITY CLASSIFICATION OF THIS PAGE

## REPORT DOCUMENTATION PAGE

| | |
|---|---|
| 1a. REPORT SECURITY CLASSIFICATION<br>UNCLASSIFIED | 1b. RESTRICTIVE MARKINGS |
| 2a. SECURITY CLASSIFICATION AUTHORITY | 3 DISTRIBUTION/AVAILABILITY OF REPORT<br>Approved for public release; distribution is unlimited. |
| 2b. DECLASSIFICATION/DOWNGRADING SCHEDULE | |
| 4. PERFORMING ORGANIZATION REPORT NUMBER(S)<br>CARDIVNSWC-TR-95/010 | 5. MONITORING ORGANIZATION REPORT NUMBER(S) |
| 6A. NAME OF PERFORMING ORGANIZATION<br>Carderock Division<br>Naval Surface Warfare Center<br>6b. OFFICE SYMBOL (If applicable)<br>Code 544 | 7a. NAME OF MONITORING ORGANIZATION |
| 6c. ADDRESS (City, State, and ZIP Code)<br>Bethesda, MD 20084-5000 | 7b. ADDRESS (CITY, STATE, AND ZIP CODE) |
| 8a. NAME OF FUNDING/SPONSORING ORGANIZATION<br>Coastal Systems Station<br>6b. OFFICE SYMBOL (If applicable)<br>Code 2720 | 9. PROCUREMENT INSTRUMENT IDENTIFICATION NUMBER |
| 8c. ADDRESS (City, State, and ZIP code)<br>Coastal Systems Station<br>Dahlgren Division, Naval Surface Warfare Center<br>6703 West Highway 98<br>Panama City, FL 32407-7001 | 10. SOURCE OF FUNDING NUMBERS<br>PROGRAM ELEMENT NO. 11221N<br>PROJECT NO. WX00103<br>TASK NO.<br>WORK UNIT ACCESSION NO. DN500257 |

11. TITLE (Include Security Classification)
A Postswirl Propulsor for a Small Vehicle

12. PERSONAL AUTHOR(S)
Chen, Benjamin Y.-H. and Tseng, Carol L.

| 13a. TYPE OF REPORT | 13b. TIME COVERED | 14. DATE OF REPORT (Year, Month, Day) | 15. PAGE COUNT |
|---|---|---|---|
| Final | FROM 6/90 TO 10/90 | 1995, April | 30 |

16. SUPPLEMENTARY NOTATION The main text of this report was presented at the Symposium of Propellers/Shafting '94, Virginia Beach, Virginia, 20-21 Sep 1994.

| 17. COSATI CODES | | | 18. SUBJECT TERMS (Continue on Reverse If Necessary and Identity by Block Number) |
|---|---|---|---|
| FIELD | GROUP | SUB-GROUP | Torque Balanced Postswirl Propulsors, Small Vehicle |
| | | | |
| | | | |

19. ABSTRACT (Continue on reverse if necessary and identify by block number)

A novel postswirl (PS) propulsor designed for a small vehicle is addressed. The major benefit of this design is the simplicity of the machinery arrangement. The challenge of this design is the low value of Reynolds number which may cause flow separation on the propulsor blade surfaces. Open-water and self-propulsion experimental results show that the performance predictions agree well with the measurements.

| 20. DISTRIBUTION/AVAILABILITY OF ABSTRACT | 21. ABSTRACT SECURITY CLASSIFICATION | |
|---|---|---|
| ☒ UNCLASSIFIED/UNLIMITED ☐ SAME AS RPT. ☐ DTIC USERS | UNCLASSIFIED | |
| 22a. NAME OF RESPONSIBLE INDIVIDUAL<br>Benjamin Y.-H. Chen | 22b. TELEPHONE (Include Area Code)<br>(301) 227-1450 | 22c. OFFICE SYMBOL<br>Code 544 |

DD FORM 1473, 84 MAR

UNCLASSIFIED

SECURITY CLASSIFICATION OF THIS PAGE

## CONTENTS



## FIGURES

## TABLES

## NOMENCLATURE

| | |
|---|---|
| $c/D$ | Chord to diameter ratio |
| $C_{Th}$ | Thrust loading coefficient |
| $D_r$ | Rotor diameter |
| $D_s$ | Stator diameter |
| $EAR$ | Expanded area ratio |
| $f_m/c$ | Maximum camber to chord length ratio |
| $G$ | Nondimensional circulation |
| $i_t/D$ | Total rake to diameter ratio |
| $K_Q$ | Torque coefficient |
| $K_T$ | Thrust coefficient |
| $N_r$ | Rotor RPM |
| $P/D$ | Pitch to diameter ratio |
| $Q$ | Torque |
| $r$ | Rotor |
| $s$ | Stator |
| $t$ | Thrust deduction fraction |
| $t/c$ | Thickness to chord ratio |
| $T$ | Thrust |
| $x$ | Axial separation between the rotor and stator |
| $X_R$ | Nondimensional radius measured from the shaft axis |
| $X_{Rh}$ | Nondimensional hub radius |
| $Z$ | Blade number |
| $\beta_i$ | Hydrodynamic pitch angle |
| $\theta_s$ | skew angle |
| $\omega$ | Angular velocity |
| $\Gamma$ | Circulation |

All other notation in this report is in accordance with the International Towing Tank Conference (ITTC) Standard Symbols.*

* "International Towing Tank Conference Standard Symbols 1976," The British Ship Research Association, BSRA Technical Memorandum No. 500 (May 1976).

THIS PAGE INTENTIONALLY LEFT BLANK

## ABSTRACT

*A novel postswirl (PS) propulsor designed for a small vehicle is addressed. The major benefit of this design is the simplicity of the machinery arrangement. The challenge of this design is the low value of Reynolds number which may cause flow separation on the propulsor blade surfaces. Open-water and self-propulsion experimental results show that the performance predictions agree well with the measurements.*


## ADMINISTRATIVE INFORMATION


This work was carried out at the Carderock Division, Naval Surface Warfare Center, and was supported by the Naval Coastal Systems Center under work request number WX00103.


## INTRODUCTION

One of the operating problems for a small vehicle is the achievement of torque balance when a vehicle is propelled by a propulsor. In some cases, contrarotating (CR) propellers have been adopted to eliminate the problem. However, in spite of the hydrodynamic benefits of CR propellers, the complex shafting and gearing arrangements have restricted the CR propeller applications.

In order to realize some of the advantages of CR propellers, without the mechanical complexity, a novel postswirl (PS) propulsor was designed for a small vehicle in the current study. A PS propulsor consists of a forward rotor and aft stator vanes. PS propulsors exhibit many advantages in terms of powering and cavitation over single (SR) propellers (Chen[1]). The improvements in the propulsive efficiency result from reduced rotation losses and axial kinetic energy losses in the propeller slipstream. The improvements in the cavitation inception speed are due to reduced blade loading for blade surface cavitation and reduced tip circulation for tip vortex cavitation. In addition to the improvement of powering and cavitation, PS propulsors can provide better stability due to torque balance generated by the rotor and stator.

The purpose or the major benefit of this design is to simplify the machinery arrangement but still provide torque balance for the vehicle. The low value of Reynolds number which may cause flow separation on the propulsor blade surfaces presents a challenge for the current design.

## SUMMARY OF POSTSWIRL PROPULSOR DESIGN METHOD

A summary of the postswirl (PS) propulsor design method is presented in this section. A detailed description of the design procedure has been presented by Chen.[1]

### DESIGN PRINCIPLE

Three fundamental principles need to be satisfied: momentum, mass, and circulation conservation. Momentum conservation requires the net force generated by the PS propulsor to be balanced by the barebody drag and the drag due to the propulsor-hull interactions. Mass conservation determines the circulation distribution of the stator once the rotor circulation is specified. Circulation conservation determines the magnitude of the circulation distribution of the stator once the rotor circulation magnitude is specified.

### DESIGN PROCEDURE

The design procedure consists of three phases: specification of operating conditions, design, and analysis. In the first phase, the design requirements and wake survey data need to be provided. The effects of the hull configuration on the flow and the hull-propulsor interaction are traditionally represented by the nominal wake and two interaction coefficients: the thrust deduction and the wake

fraction. In the current design, panel and boundary layer methods were employed to determine the vehicle resistance and the propulsor inflow boundary layer profile because there were no measured data.

The design phase consisted of three parts. The preliminary design stage used lifting-line theory to perform a parametric study to determine optimum rotor and stator diameters, rotation speed, and numbers of blades. Circulation distributions for the rotor and stator were also determined in this phase. Propulsive efficiency and cavitation were considered in the decisions made during this design phase.

In the intermediate design phase, cavitation inception and strength were the major factors guiding the choice of thickness, chord length, and blade loading distributions for the rotor and stator. Consideration was also given to strength requirements and propulsive efficiency which were effected by these design parameters. Blade surface cavitation and tip vortex cavitation calculations were performed for both rotor and stator.

The final design stage consisted of using lifting-surface theory to incorporate three dimensional effects in the design. This stage includes determining pitch and camber distributions. In the analysis phase, steady and unsteady forces and moments were calculated.

## POSTSWIRL PROPULSOR DESIGN

### DESIGN GUIDELINES

The PS propulsor design for the small vehicle sought to maximize propulsive efficiency while minimizing propulsor noise due to cavitation and unsteady forces. The design also provides sufficient cancellation of the rotor torque by the stator for stability. During the design process, the designers strove to provide a design that would deliver cavitation-free operation at the operating conditions and residual torque within the requirements for stability.

### DESIGN REQUIREMENTS

There were several constraints placed on the design due to the limitations of the device. The thrust loading coefficient, $C_{TH}$ was 0.7529. The ratio of the rotor diameter to the maximum vehicle diameter was restricted to 0.96. The machinery limitations dictated that the maximum shaft horsepower available was 6.7 hp and the rotation speed was set at 3500 rpm. The residual rotor torque was to be less than 2 ft-lb to minimize the angle of attack on the control surfaces.

### DESIGN RISK AREAS

Four risk areas cast some uncertainty on the performance of this design. They include low Reynolds number, low aspect ratio, high acoustic noise, and unknown resistance and wake.

- *Low Reynolds number risk*: Due to the small size of the propulsor, the Reynolds number at the maximum speed is $0.72 \times 10^6$ for the rotor and is $0.33 \times 10^6$ for the stator. At the minimum operating speed, the Reynolds number drops to $0.40 \times 10^6$ for the rotor and $0.19 \times 10^6$ for the stator. At these low Reynolds numbers it was uncertain whether or not the propulsor would be operating in turbulent or laminar flow. If the flow was laminar, the drag coefficient would decrease and the rotation speed would increase as would the propulsive efficiency.

- *Low aspect ratio risk*: The large chord lengths on the rotor and the stator produce blades with low aspect ratios. The aspect ratio of the rotor blades was 1.12 and the stator blades was 0.80. These low aspect ratios produced a risk of flow separation resulting in stall situation.

- *High acoustic noise risk*: The high rotation speed of the rotor (3500 rpm) can cause blade rate noise and broadband vibration noise. Unfortunately, the constraints of the motor dictated the choice of the rotation speed and a lower speed could not be chosen.

• *Unknown resistance and wake risk*: The final concern was the uncertainty of the resistance, wake, and interaction coefficients. Since there were no model test results available, the resistance, wake, thrust deduction, and wake fraction were estimated from other sources. Deviations of these estimates from the actual values would affect the performance of the propulsor. The above risk areas made this design challenging.

## RESISTANCE AND WAKE INFORMATION

As was mentioned before, the propulsor design started prior to building the vehicle. Therefore, the propulsor designers had to use other sources to obtain the following information:

• A resistance and a mean velocity profile for the flow at the rotor and stator planes for powering calculations.

• A circumferential velocity distribution at the rotor and stator planes for blade surface cavitation analysis.

The resistance of the propelled body and the mean velocity profile of the flow at the rotor and stator planes were calculated using a boundary layer code developed by Huang, et al.[2] The calculated mean velocity profile was compared with available experimental data from other similar axisymmetric bodies. The calculated circumferential velocity distribution was obtained by scaling the experimental data from the similar axisymmetric bodies to match the mean velocity profile of this small vehicle.

The thrust deduction factor of 0.86 was calculated using a panel code, with and without an actuator disk, developed by Maskew.[3] A sensitivity study on the effect of variation of thrust deduction on the propulsor performance was done using inverse lifting surface calculations. One case examined increasing the thrust deduction to 0.94 which resulted in a 3 percent decrease in the rotation speed. The second case examined decreasing the thrust deduction to 0.80 which resulted in a 2 percent increase in the rotation speed.

Using the effective wake calculation procedure by Huang, et al.,[4] a wake fraction of 0.85 was calculated. The interaction coefficients from similar axisymmetric bodies were compared with the small vehicle. The results show that the estimates for the small vehicle interaction coefficients were reasonable.

## PARAMETRIC STUDY

The design parameters for the present study were chosen based on a parametric study. The stator diameter was determined through mass conservation. To ensure that the stator operates inside the tip vortices of the rotor, the final stator diameter, which is 85 percent of the rotor diameter, was chosen to be slightly smaller than the preliminary diameter calculated using mass conservation. The axial spacing was chosen to be 40 percent of the rotor diameter. A summary of the design parameters for the PS propulsor design is given in Table 1.

**Table 1.** PS propulsor design - summary.

| Design Characteristics | Rotor | Stator |
|---|---|---|
| $(V_S)_{design}/(V_S)_{minimum}$ | 1.73 | 1.73 |
| Rotational speed (rpm) | 3,500 | 0 |
| Thrust loading coefficient | 0.7529 | |
| Geometry | | |
| Diameter / max vehicle dia. | 0.96 | 0.815 |
| Number of blades | 9 | 13 |
| Expanded area ratio | 0.723 | 1.924 |
| Skew (deg) | 30 | 0 |
| Total rake | 0 | 0 |
| Blade sections | * | * |
| Axial spacing/rotor dia. | 0.40 | |

* NACA 66 (TMB Modified) Thickness
NACA a = 0.8 Meanline

## PRELIMINARY DESIGN

In the preliminary design phase, the following considerations were incorporated:

- Residual torque less than 2.0 ft-lb.
- Lift coefficient $C_L \leq 0.2$ to minimize possibility of flow separation.
- Blade number choice for unsteady forces.

Lifting-line calculations were used in this part of the design in determining the circulation distributions for the rotor and the stator. The lifting-line theory developed by Kerwin et al.[5] was employed in the current study. Although the Reynolds number is small ($0.72 \times 10^6$ for rotor blade and $0.33 \times 10^6$ for stator blade), it was assumed that a fully turbulent flow exists on the blade surfaces.

The optimum circulation distribution for the rotor was used and the circulation distribution for the stator was adjusted to maximize torque cancellation. The stator was designed to cancel 90 percent of the rotor torque. The residual torque of 1 ft-lb was balanced by the control surfaces. To ensure no tip vortex cavitation for both the rotor and stator, the circulation at the rotor and stator tip was unloaded although the large chord length and the low lift coefficient produced a low circulation at the tip. Figure 1 shows the circulation distribution for the rotor and the stator.

The number of blades chosen was 9 for the rotor and 13 for the stator. The large blade numbers were necessary to bring the lift coefficient on the blades below 0.2. The guideline of keeping the lift coefficient under 0.2 was followed because the propulsor will operate at a very low Reynolds number and there is a danger of flow separation occurring which will cause thrust loss on the rotor and torque loss on the stator. The chord-length distributions for the rotor and the stator were also chosen to reduce the lift coefficient which is why the expanded area ratio, EAR, is so large. Unfortunately the large chord lengths and large blade numbers increased the drag which in turn reduced the propulsive efficiency.

## INTERMEDIATE DESIGN

In the intermediate design, a thickness distribution for the rotor and the stator was chosen based on strength and cavitation calculations. The material chosen for the propulsor was marine grade 7075 aluminum. The strength requirement at the full power condition was not to exceed 12,500 psi. Stress calculations for the rotor and the stator were performed using a simple beam theory (Schott et al.[6]).

The blade surface cavitation calculations were performed using a two-dimensional airfoil theory developed by Brockett.[7] The thickness distribution could have been reduced drastically for both the rotor and the stator because the strength and cavitation performance of both components exceeded the requirements. However, due to manufacturing constraints, the thickness could not be reduced.

## FINAL DESIGN

The final pitch and camber distributions were determined using the lifting-surface program developed by Wang[8] with hub effects included. The induced velocities on the stator were calculated from the lifting-line calculation. An a = 0.8 meanline loading was used and a modified NACA 66 thickness form was used.

Figure 2 shows the pitch distribution for the rotor as calculated from the lifting-surface calculation and the final faired pitch distribution. Figure 3 shows the pitch angle distribution for the stator as calculated from the lifting-surface calculation and the final faired pitch angle distribution. Figure 4 shows the final camber distributions for the rotor and the stator from the lifting-surface calculations.

## STEADY AND UNSTEADY FORCE ANALYSIS

Steady force predictions for the design condition at the maximum speed and off-design conditions at the minimum speed were performed using the inverse lifting-surface theory. The vortex lattice method including hub effects, developed by Greeley and Kerwin[9] was employed.

Efforts to minimize unsteady forces included the blade number selection and the addition of skew to the rotor. The blade number combination was chosen to minimize unsteady forces according to work by Strasberg and Breslin.[10] A non-linear skew distribution with thirty degrees skew at the tip was selected for the rotor. Unsteady force predictions for the rotor were performed using the propeller unsteady force theory developed by Kerwin and Lee.[11]

# PERFORMANCE PREDICTION AND EXPERIMENTAL RESULTS

Aluminum models of the rotor and stator were manufactured based on the final design geometry. The self-propulsion tests were carried out using DTRC model propeller 5153 to represent the rotor and model propeller 5154 to represent the stator. The open-water and self-propulsion tests were performed at DTRC.

## OPEN-WATER TESTS

Figure 5 shows the test results for the PS propulsor as a function of advance coefficient and the performance prediction at the design advance coefficient. The predicted and measured performance of the PS propulsor design is shown in Table 2.

**Table 2.** Predicted and measured open-water performance of PS propulsor design.

| | Measurement | Inverse Calculation for Uniform Inflow | |
|---|---|---|---|
| | Open-Water Experiment | Turbulent Flow | Laminar Flow |
| $J_A$ | 0.815 | 0.818 | 0.825 |
| $K_T$ | 0.1963 | 0.1978 | 0.2012 |
| $K_Q$ | 0.0401 | 0.0438 | 0.0370 |
| $\eta_o$ | 0.635 | 0.588 | 0.714 |

Because there was no flow visualization on the blade surface, inverse calculations for uniform flow were conducted to evaluate the self-propelled flow situation. At constant $C_{TH}$, the open-water measurements of thrust, torque, advance coefficient, and efficiency are within the turbulent flow and laminar flow predictions.

## SELF-PROPULSION TESTS

Figure 6 shows the measured delivered power and rotation speed of the unit as a function of ratio of vehicle speed as well as the predicted performance at the design ratio of vehicle speed. Table 3 shows the predicted and measured self-propulsion performance at the design ratio of vehicle speed of the PS propulsor.

The calculated effective horsepower used in the design is almost identical to the measurement. The thrust deduction and the wake fraction were never obtained because the rotor thrust measurement was not reliable. This results from using the subminiature load cells instead of a dynamometer to measure rotor thrust. The designed advance coefficient or the designed rotation speed is 1.2 percent higher than the measurement. The designed residual rotor torque is 0.5 ft-lb higher than the measured value.

As in the open-water experiments, no flow visualization on the blade surface was performed in the self-propulsion tests. Inverse calculations at the measured advance coefficient were carried out. The measured thrust, torque, delivered horsepower, and efficiency are within the turbulent flow and laminar flow predictions.

In general, the accuracy of the experimental measurements with the PS propulsor is $\pm$ 2 percent. Overall the predicted values agree well with the experimental measurements, and in general are within the accepted accuracy of the experimental measurements. Views of the PS propulsor created on a Computer Vision system are shown in Figure 7.

**Table 3.** Predicted and measured self-propulsion performance of PS propulsor design.

| | Design | Measurement | Inverse Calculation at Measured Advanced Coefficient | |
|---|---|---|---|---|
| | | Self-propulsion Experiment | Turbulent Flow | Laminar Flow |
| $(V_S)$design | 1.73 | 1.73 | 1.73 | 1.73 |
| $(V_S)$minimum | | | | |
| $P_E$ (hp) | 4.1 | 4.1 | 4.1 | 4.1 |
| $P_D$ (hp) | 6.4 | 5.8 | 6.1 | 5.2 |
| 1-t | 0.86 | --- | 0.86 | 0.86 |
| $1-w_T$ | 0.848 | --- | 0.848 | 0.848 |
| $J_S$ | 1.002 | 1.013 | 1.013 | 1.013 |
| N (rpm) | 3,500 | 3,460 | 3,460 | 3,460 |
| $T_{rotor}$ (lb) | 89.1 | --- | 84.9 | 88.1 |
| $Q_{rotor}$/ft-lb) | 9.6 | 8.8 | 9.2 | 7.9 |
| $T_{stator}$(lb) | 1.4 | --- | -1.0 | 1.5 |
| $Q_{stator}$(ft-lb) | 8.6 | 8.3 | 8.4 | 8.4 |
| $\eta_D$ | 0.64 | 0.70 | 0.67 | 0.78 |

## CONCLUSIONS

The following conclusions can be drawn from the present study.

1. Despite the four risk areas (low Reynolds number, low aspect ratio, high acoustic noise, and unknown resistance and wake), the PS propulsor design met all of the design requirements.

2. The predicted resistance matched well with the measured resistance. This may indicate a good agreement between predicted and actual wake data which was never measured.

3. Unfortunately measured hull-propulsor interaction coefficients were not available. The predicted hull-propulsor interaction coefficients may be very close to the actual value due to the good performance of the propulsor.

4. Although there was no flow visualization on the blade surface, the inverse calculations together with the open-water and self-propulsion measurements indicate that the flow on the blade surface is partially laminar and partially turbulent.

5. The measured residual rotor torque was 0.5 ft-lb which results in the angle of attack of the control surface to adjust less than 2 degrees to counter-balance the residual torque. In other words, this novel PS propulsor design has achieved the goal of the simplicity of the machinery arrangement as opposed to the complex shafting and gearing arrangements of the CR propellers. However, it still provide sufficient torque balance for the small vehicle.

## ACKNOWLEDGMENT

The authors would like to thank Mr. G. Hampton and Mr. Ray Cross for carrying out the open-water and self-propulsion experiments.

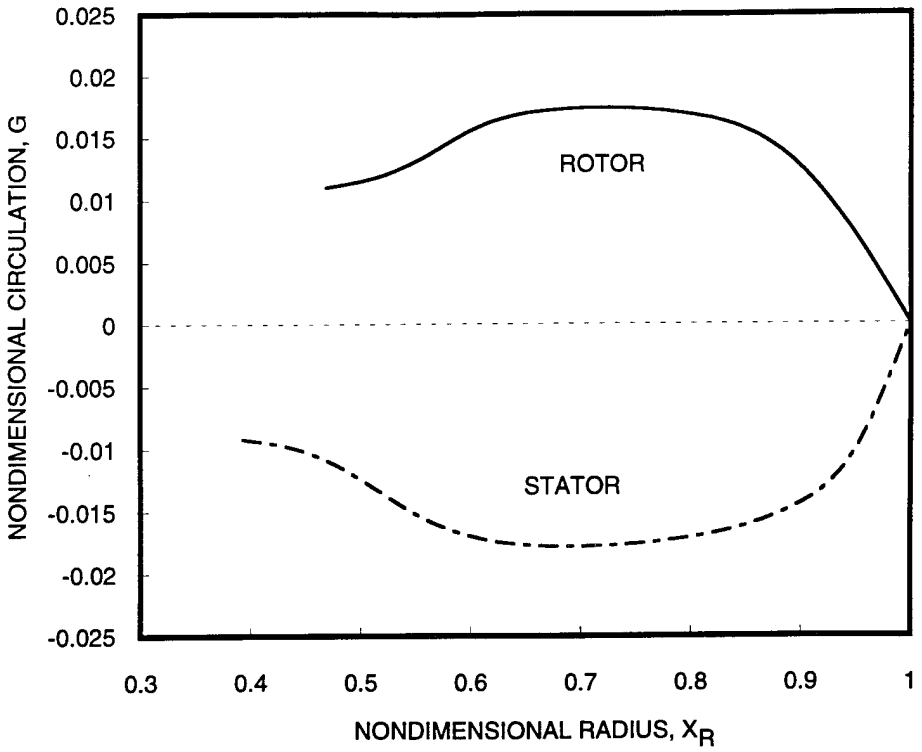


**Fig. 1.** Circulation distribution for rotor and stator.

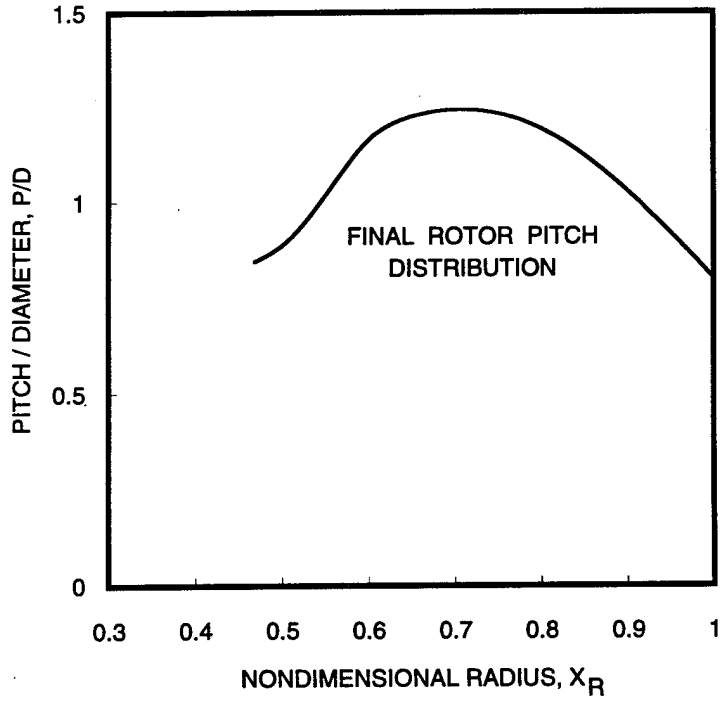


**Fig. 2.** Final pitch to diameter ratio for rotor.

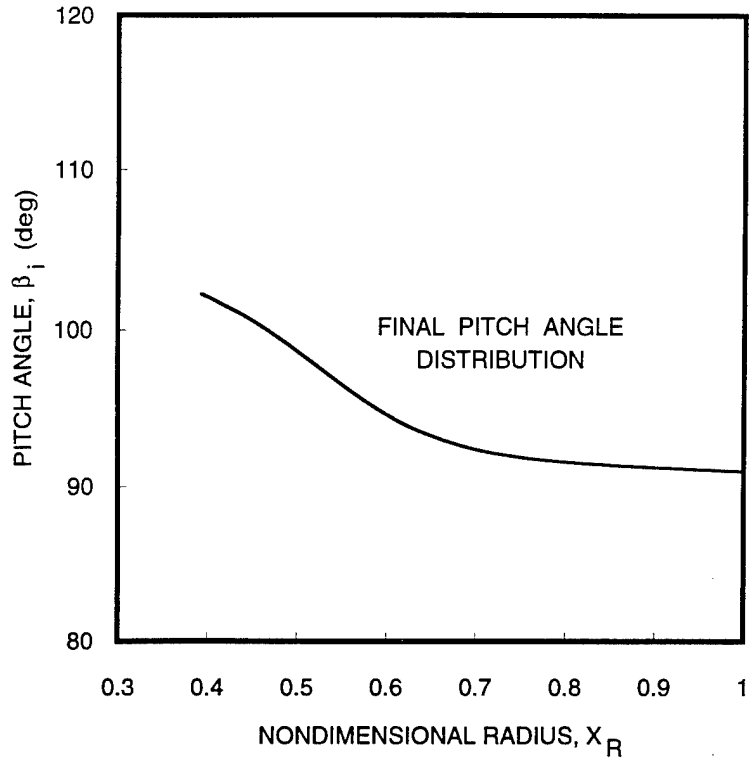


**Fig. 3.** Final hydrodynamic pitch angle for stator.

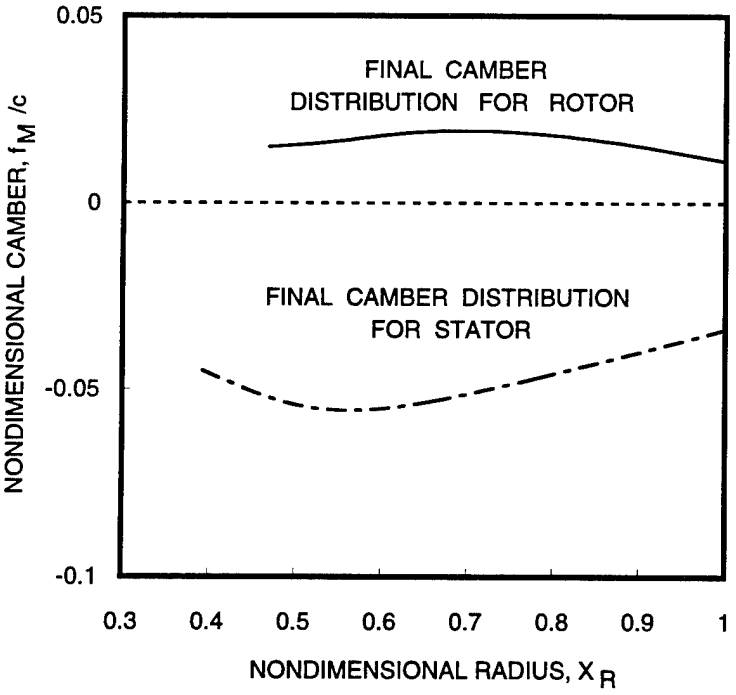


**Fig. 4.** Final maximum camber to chord length ratio distribution.

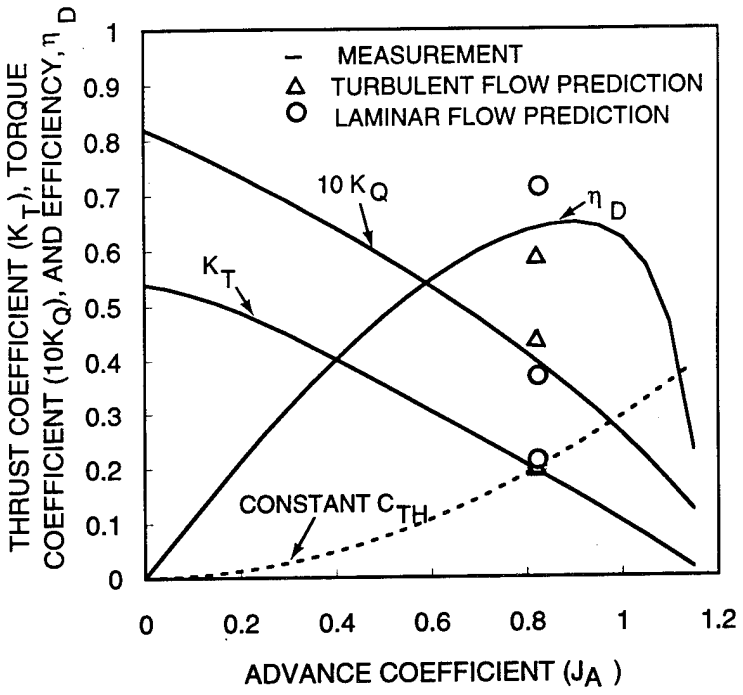


**Fig. 5.** Predicted and measured open-water test results.

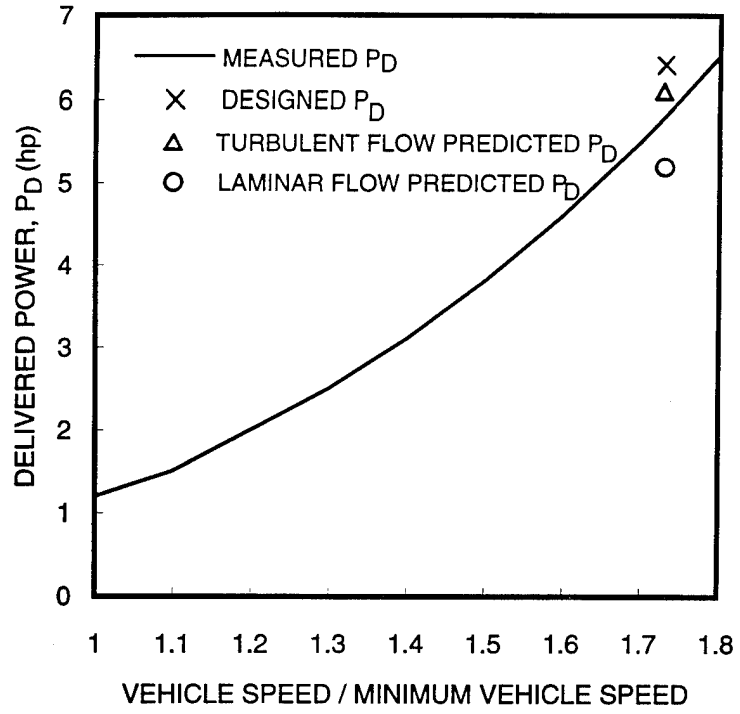


**Fig. 6a.** Delivered power.

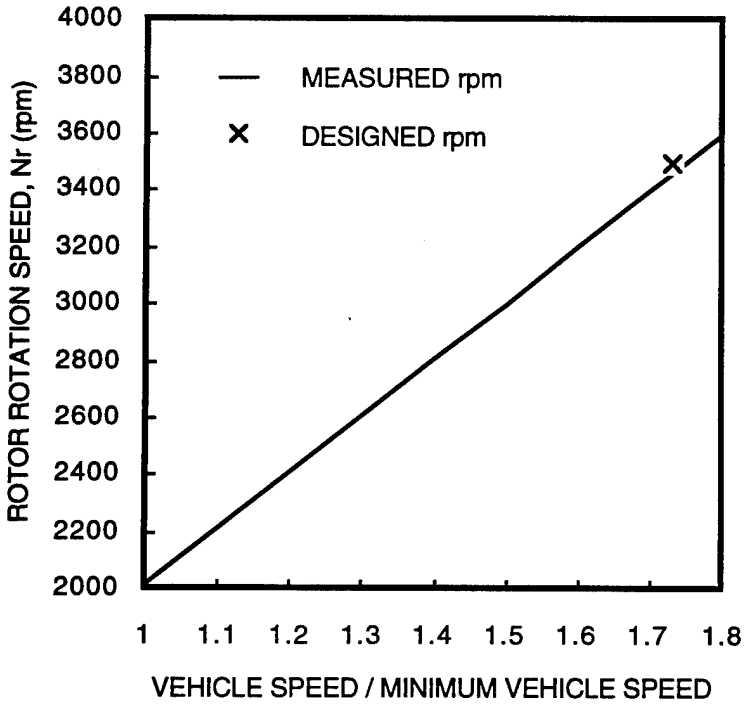


**Fig. 6b.** Rotation speed.

**Fig. 6.** Predicted and measured self-propulsion test results.

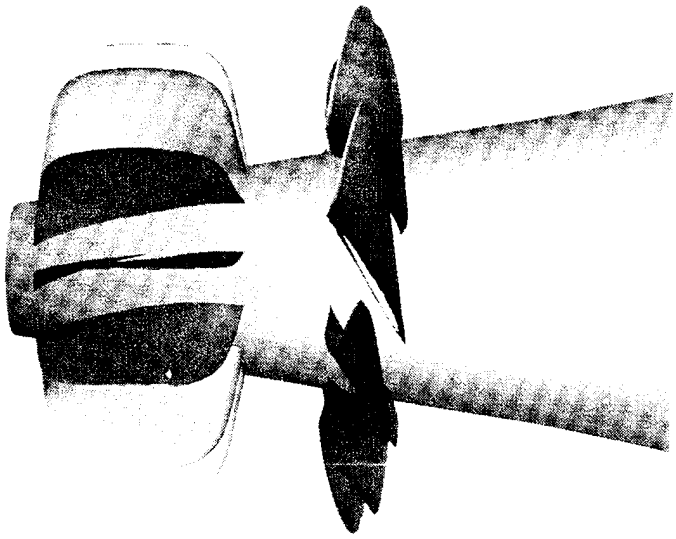

**Fig. 7a.** Side view.

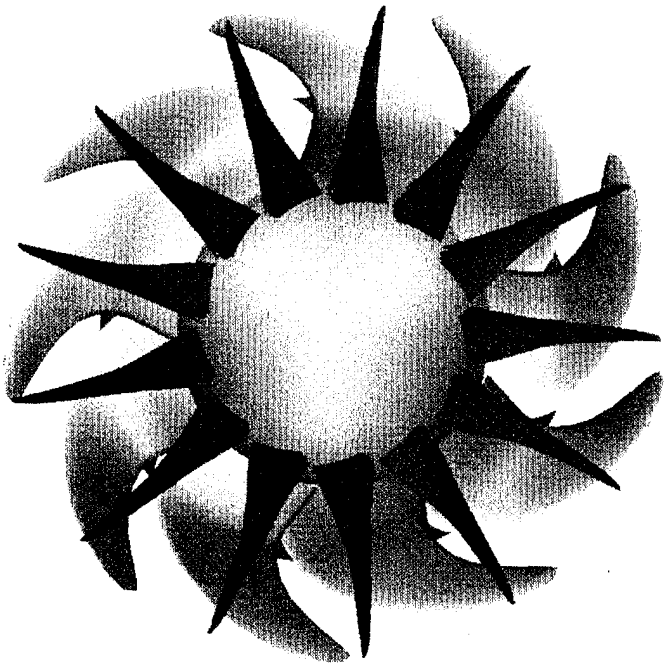

**Fig. 7b.** Stern view.

**Fig. 7.** Views of postswirl propulsor.

**THIS PAGE INTENTIONALLY LEFT BLANK**

## APPENDIX

This section provides additional information for the original paper. The chord-length distributions of the rotor and stator were chosen, based on cavitation, flow separation, and efficiency considerations. The chord distributions for the rotor and stator are shown in Figure A.1.

The thickness distribution was selected based on strength and cavitation considerations. Figure A.2 shows the thickness distributions for the rotor and stator.

As shown in Figure A.3, a tip skew distribution of 25 degrees, varying nonlinearly from zero at the hub, was selected for the rotor. The stator was designed with zero skew. The total rake for both rotor and stator was zero. Therefore, the rotor has negative rake to offset the skew-induced rake. The stress distributions computed by beam theory corresponding to these choices of geometry are given in Figure A.4.

The final geometric specifications of the PS propulsor, including the details of the leading and trailing edges were computed using the computer code, XYZ-PROP, developed by Brockett.[12] All the input data, such as chord length, thickness, skew, pitch, and camber distributions, were faired by a cubic spline procedure before being input to XYZ-PROP; see Table A.1.

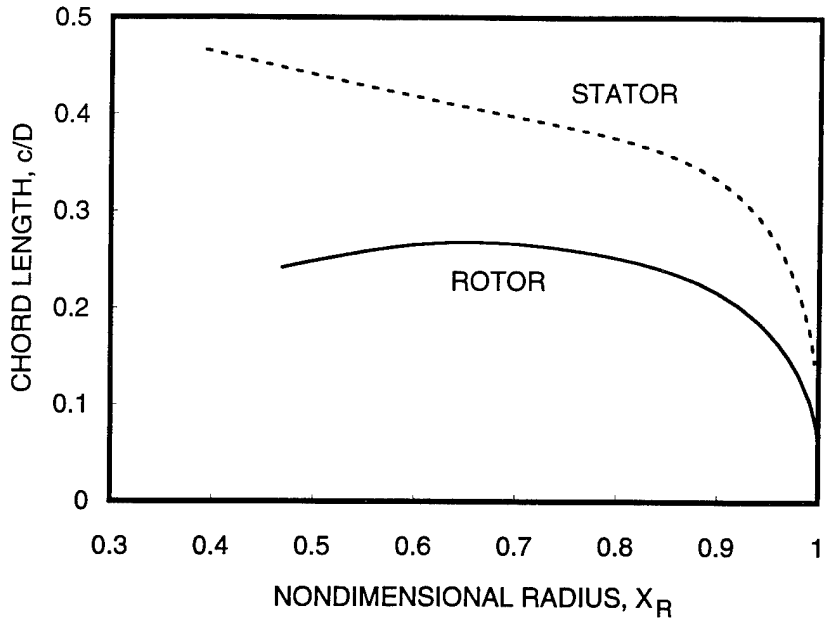


**Fig. A.1.** Radial distribution of chord length.

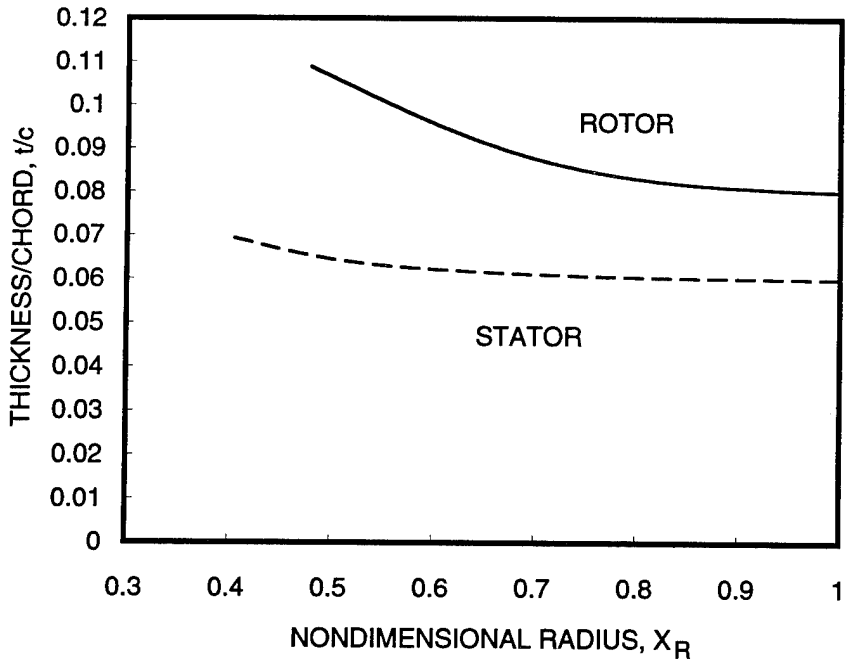


**Fig. A.2.** Radial distribution of thickness.

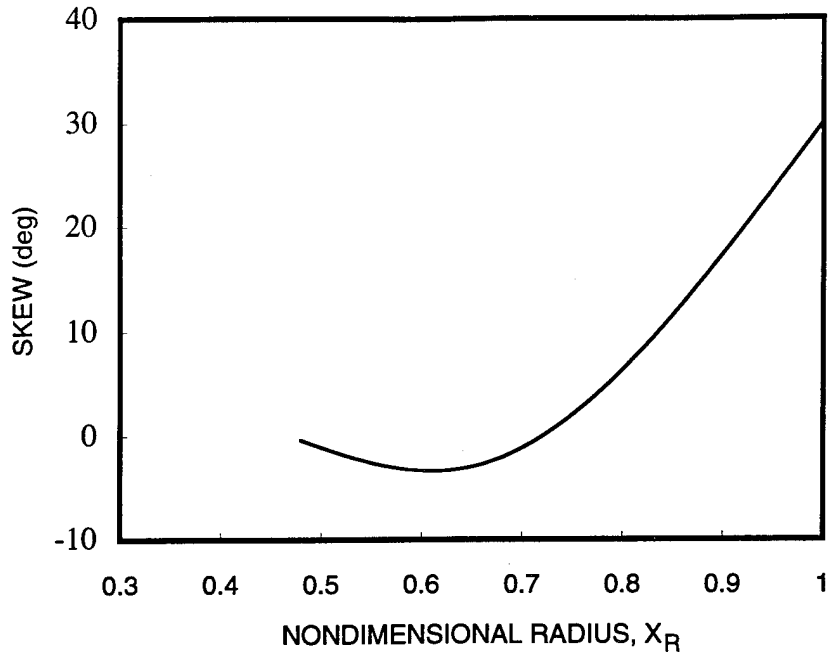


**Fig. A.3.** Radial distribution of skew.

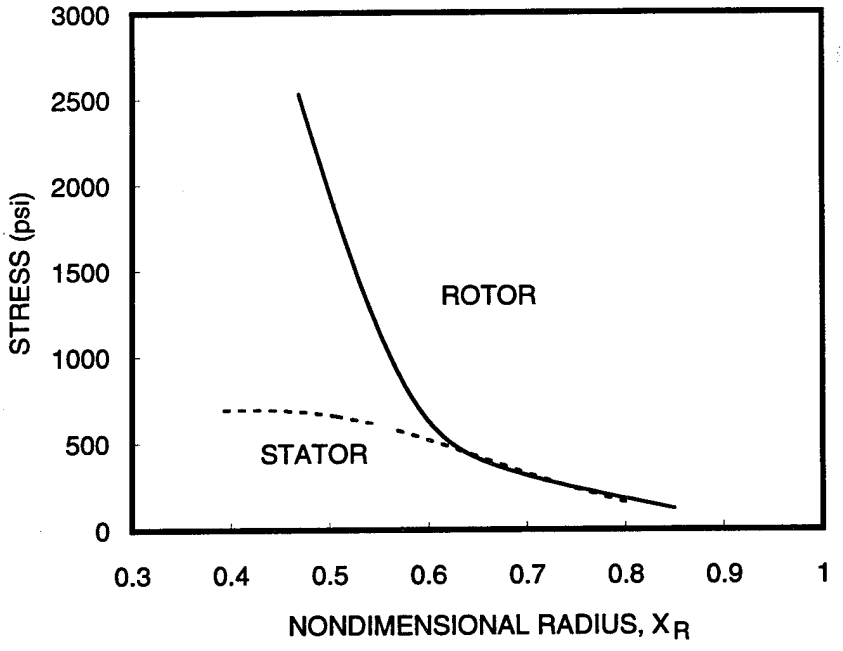


**Fig. A.4.** Radial distribution of stress.

**Table A.1.** Final design geometry for PS propulsor.

**Table A.1a.** Rotor.

| r/R | c/D | P/D | $i_T$/D | $\theta_s$ | t/c | $f_m$/c |
|---|---|---|---|---|---|---|
| 0.4688 | 0.24190 | 0.8800 | 0.0000 | 0.00000 | 0.11000 | 0.01590 |
| 0.5000 | 0.24870 | 0.9160 | 0.0000 | -1.08800 | 0.10650 | 0.01649 |
| 0.5500 | 0.25850 | 1.0200 | 0.0000 | -2.57100 | 0.10100 | 0.01750 |
| 0.6000 | 0.26499 | 1.1500 | 0.0000 | -3.35200 | 0.09580 | 0.01855 |
| 0.6500 | 0.26761 | 1.2240 | 0.0000 | -3.00000 | 0.09130 | 0.01947 |
| 0.7000 | 0.26630 | 1.2210 | 0.0000 | -1.19200 | 0.08770 | 0.02000 |
| 0.8000 | 0.25145 | 1.1350 | 0.0000 | 6.22400 | 0.08310 | 0.01927 |
| 0.8500 | 0.23730 | 1.0600 | 0.0000 | 11.38500 | 0.08180 | 0.01810 |
| 0.9000 | 0.21560 | 0.9600 | 0.0000 | 17.21700 | 0.08100 | 0.01648 |
| 0.9500 | 0.17500 | 0.8340 | 0.0000 | 23.49700 | 0.08040 | 0.01456 |
| 1.0000 | 0.05000 | 0.6800 | 0.0000 | 30.00000 | 0.08000 | 0.01250 |

**Table A.1b.** Stator.

| r/R | c/D | $\phi_P$ | $i_T$/D | $\theta_s$ | t/c | $f_m$/c |
|---|---|---|---|---|---|---|
| 0.3931 | 0.46600 | 101.8000 | 0.0000 | 0.0000 | 0.07000 | -0.04500 |
| 0.4500 | 0.45252 | 100.1000 | 0.0000 | 0.0000 | 0.06678 | -0.05053 |
| 0.5000 | 0.44080 | 96.0080 | 0.0000 | 0.0000 | 0.06450 | -0.05410 |
| 0.5500 | 0.42930 | 94.0970 | 0.0000 | 0.0000 | 0.06306 | -0.05558 |
| 0.6000 | 0.41810 | 92.7370 | 0.0000 | 0.0000 | 0.06220 | -0.05525 |
| 0.6500 | 0.40740 | 93.8499 | 0.0000 | 0.0000 | 0.06157 | -0.05364 |
| 0.7000 | 0.39710 | 91.8750 | 0.0000 | 0.0000 | 0.06108 | -0.05130 |
| 0.8000 | 0.37470 | 91.0690 | 0.0000 | 0.0000 | 0.06045 | -0.04592 |
| 0.9000 | 0.33150 | 90.6950 | 0.0000 | 0.0000 | 0.06014 | -0.04003 |
| 0.9500 | 0.28000 | 90.5640 | 0.0000 | 0.0000 | 0.06006 | -0.03968 |
| 1.0000 | 0.07500 | 90.4500 | 0.0000 | 0.0000 | 0.06000 | 0.03390 |

## REFERENCES


1. Chen, B.Y.-H., "Postswirl Propulsors - A Design Method and An Application," *International Symposium on Propulsors and Cavitation*, Hamburg, Germany (1992).

2. Huang, T.T., N. Santelli, and G. Belt, "Stern Boundary-Layer Flows on Axisymrnetric Bodies," *12th Symposium on Naval Hydrodynamics*, Washington, DC, pp.127-147 (1978).

3. Maskew, B., "A Computer Program for Calculating the nonlinear Aerodynamic Characteristics of Arbitrary Configurations," Analytic Methods, Inc. (1982).

4. Huang, T.T., N. Santelli, and N.C. Groves, "Propellers/Stern/Boundary-Layer Interaction on Axisymmetric Bodies: Theory and Experiment," Ship Performance Department, DTRC, Report 76-0113 (Dec 1976).

5. Kerwin, J.E., W.B. Conney and C.-Y. Hsin, "Optimum Circulation Distributions for Single and Multiple-Component propulsors," *21st American Towing Tank Conference*, Washington DC (1986).

6. Schott, C.G., J. McMahon, P. Hargrove, and N. Hubbard, "A Computer Code the for the Prediction of Propeller Blade Stress by Cantilever Beam Theory," Ship Hydromechanics Departmental Report, DTRC-SHD-1151-23 (Mar 1989).

7. Brockett, T., "Minimum Pressure Envelopes for Modified NACA 66 Sections with NACA a=0.8 Camber and BUSHIPS Type I and II Sectlons," David Taylor Model Basin Report 1780, (Feb 1966).

8. Wang, M.H., "Hub Effects in Propeller Design and Analysis," Department of Ocean Engineering, MIT Report 85-14 (1985).

9. Greeley, D.S. and J.E. Kerwin, "Numerical Methods for Propeller Design and Analysis in Steady Flow," *Transactions SNAME*, Vol. 90 (1982).

10. Strasberg, M. and J.P. Breslin, "Frequencies of the Alternating Forces due to Interactions of Contrarotating Propellers," *Journal of Hydronautic*, Vol. 10, No. 2 (Apr 1976).

11. Kerwin, J.E., and C.S. Lee, "Prediction of Steady and Unsteady Marine Propeller Performance by Numerical Lifting-Surface Theory," *SNAME Transactions*, Vol. 86 (1978).

12. Brockett, T.E., "Analytical Specification of Propeller Blade-Surface Geometry," DTRC Ship Hydrodynamics Department Report, DTRC/SHD-699-01 (1976).

THIS PAGE INTENTIONALLY LEFT BLANK

# INITIAL DISTRIBUTION

| Copies | Code | Name |
|---|---|---|
| 2 | CNO | |
| | 1 | N87T |
| | 1 | N87T2 |
| 2 | ONR | |
| | 1 | 344 R. Vogelsong |
| | 1 | 344 P. Majumdar |
| 1 | ONR Boston | |
| 1 | ONR Chicago | |
| 1 | ONR London, England | |
| 1 | NRL | |
| 1 | USNA/Lib | |
| 1 | NAVPGSCOL/Lib | |
| 1 | NROTC &NAVADMINU, MIT | |
| 1 | NADC | |
| 1 | NCCOSC RDT&E Div/ T. Mautner | |
| 1 | NUWCD/ J. Uhlman | |
| 6 | NAVSEA | |
| | 1 | 03D |
| | 1 | 03T |
| | 1 | 03H32 |
| | 1 | 03X1 |
| | 1 | 03X7 |
| | 1 | 03Z |
| 1 | NSWC-DGD/ K. Rose | |
| 1 | ART/ R. Gulino | |
| 2 | MMA | |
| | 1 | Lib |
| | 1 | Maritime Res Cen |
| 2 | DTIC | |
| 1 | LC/SCI & Tech Div | |
| 2 | NASA STIF | |
| | 1 | Dir Res |
| | 1 | Lib |
| 1 | NSF Engr Div/Lib | |
| 1 | DOT Lib | |

| Copies | Code | Name |
|---|---|---|
| 1 | U. Cal. Berkley/Lib | |
| 1 | CIT/AERO Lib | |
| 1 | U. Iowa/Lib | |
| 1 | U. Michigan/Lib | |
| 2 | MIT | |
| | 1 | Barker Engr Lib |
| | 1 | Ocean Engr/ J. Kerwin |
| 3 | State U. Maritime Col | |
| | 1 | ARL Lib |
| | 1 | Engr Dept |
| | 1 | Inst Math Sci |
| 3 | Penn State U. APL | |
| | 1 | Lib |
| | 1 | M. Billet |
| | 1 | D. Thompson |
| 1 | Boeing Adv Amr Sys Div | |
| 1 | Brewer Engr Lab | |
| 1 | Stanford Res Inst Lib | |
| 1 | SIT Davidson Lab/Lib | |
| 1 | Texas U. ARL Lib | |
| 1 | VPI/Dept Aero & Ocean Engr/Schetz | |
| 1 | Webb Inst/ J. Hadler | |
| 1 | WHOI Ocean Engr Dept | |
| 1 | WPI Alden Hydr Lab Lib | |
| 1 | ASME/Res Comm Info | |
| 1 | ASNE | |
| 1 | SNAME/Tech Lib | |
| 1 | Allis Chalmers, York, PA | |
| 1 | AVCO Lycoming | |
| 1 | Baker Manufacturing | |
| 2 | Bird-Johnson Co | |
| | 1 | J. Norton |
| | 1 | G. Platzer |

## INITIAL DISTRIBUTION (Continued)

| Copies | Code | Name |
|---|---|---|
| 1 | | Douglas Aircraft/Lib |
| 2 | | Exxon Res Div |
| | 1 | Lib |
| | 1 | Fitzgerald |
| 1 | | Friede & Goldman/Michel |
| 1 | | Gibbs & Cox/Lib |
| 1 | | Rosenblatt & Son/Lib |
| 1 | | Inst for Defense Anal |
| 1 | | Itek Vidya |
| 1 | | Lips Duran/Kress |
| 1 | | Littleton R & Engr Corp/Reed |
| 1 | | Litton Industries |
| 1 | | Lockeed, Palmdale/ A. Solomin |
| 1 | | Maritech, Inc./Vassilopoulis |
| 1 | | HRA/JJMA, Inc./ B. Cox |
| 1 | | AME/ O. Scherer |
| 1 | | Arete Associates/ T. Brockett |
| 1 | | Nielson Engr/Spangler |

DIVISION DISTRIBUTION

| Copies | Code | Name |
|---|---|---|
| 1 | 011 | J. Corrado |
| 1 | 0114 | K.-H. Kim |
| 1 | 3411 | Publications |
| 1 | 3421 | TIC (C) |
| 1 | 3422 | TIC (A) |
| 10 | 3432 | Reports Control |
| 1 | 50 | W. Morgan |
| 1 | 506 | D. Walden |
| 1 | 508 | R. Boswell |
| 1 | 52 | W.-C. Lin |
| 1 | 521 | W. Day |
| 1 | 522 | K. Remmers |
| 1 | 54 | B. Webster |
| 1 | 542 | T. Huang |
| 20 | 544 | B. Chen |
| 1 | 544 | C. Tseng |
| 1 | 56 | D. Cieslowski |
| 1 | 60 | G. Wacker |
| 1 | 65 | R. Rockwell |
| 1 | 70 | M. Sevik |
| 1 | 7051 | W. Blake |
| 1 | 7250 | R. Szwerc |